AIAA JOURNAL
Vol. 45, No. 8, August 2007

Vibration Analysis of Rotating Laminated Cylindrical Shells

Hsuan-Teh Hu* and Kou-Long Wang†
National Cheng-Kung University, Tainan 701, Taiwan, Republic of China

DOI: 10.2514/1.28674

Free vibration analyses of rotating laminated cylindrical shells are carried out by the ABAQUS© finite element program. The fundamental frequencies of rotating laminated cylindrical shells with a given material system are then maximized with respect to fiber orientations by using the golden section method. The significant influences of rotating speed, end conditions, shell thickness, shell length, and shell radius on the maximum fundamental frequencies and the associated optimal fiber orientations are demonstrated.

Nomenclature

$\{\boldsymbol{D}\}$	=	vector for the unrestrained nodal degrees of freedom
$[K]$	=	structural stiffness matrix
L	=	length of the shell
$[M]$	=	structural mass matrix
$\{M\} = \{M_x, M_y, M_{xy}\}^T$	=	moments for composite shell element
$\{N\} = \{N_x, N_y, N_{xy}\}^T$	=	in-plane forces for composite shell element
r	=	radius of the shell
t	=	thickness of the shell section
$\{V\} = \{V_x, V_y\}^T$	=	transverse shear forces for composite shell element
$\{\gamma\} = \{\gamma_{xz}, \gamma_{yz}\}^T$	=	transverse shear strains for a lamina in the element coordinates
$\{\gamma'\} = \{\gamma_{13}, \gamma_{23}\}^T$	=	transverse shear strains for a lamina in the material coordinates
$\{\varepsilon\} = \{\varepsilon_x, \varepsilon_y, \gamma_{xy}\}^T$	=	in-plane strains for a lamina in the element coordinates
$\{\varepsilon_0\} = \{\varepsilon_{x0}, \varepsilon_{y0}, \gamma_{xy0}\}^T$	=	in-plane strains at the midsurface of the laminate section
$\{\varepsilon'\} = \{\varepsilon_1, \varepsilon_2, \gamma_{12}\}^T$	=	in-plane strains for a lamina in the material coordinates
θ	=	angle between the material 1 axis and the element local x axis
$\{\kappa\} = \{\kappa_x, \kappa_y, \kappa_{xy}\}^T$	=	the curvatures of the laminate section
$\{\sigma\} = \{\sigma_x, \sigma_y, \tau_{xy}\}^T$	=	in-plane stresses for a lamina in the element coordinates
$\{\sigma'\} = \{\sigma_1, \sigma_2, \tau_{12}\}^T$	=	in-plane stresses for a lamina in the material coordinates
$\{\tau\} = \{\tau_{xz}, \tau_{yz}\}^T$	=	transverse shear stresses for a lamina in the element coordinates
$\{\tau'\} = \{\tau_{13}, \tau_{23}\}^T$	=	transverse shear stresses for a lamina in the material coordinates
Ω	=	rotating speed of cylindrical shell
ω	=	frequency of the shell

I. Introduction

BECAUSE of lightweight, high strength, and the flexibility of selection fiber angle to fit the requirement of design, the applications of fiber-reinforced composite laminated materials to advanced aerospace and mechanical structures have been increased rapidly in recent years. One of the important applications for fiber-reinforced composite laminated materials is the rotating cylindrical shell (or rotating shaft) such as gas turbine engines, electric motors, rotor systems, drilling pipe, etc. Because these kinds of structures are subjected to dynamic loading in service, knowledge of the dynamic characteristics of the cylindrical shells such as their fundamental natural frequencies is essential.

The fundamental natural frequency of rotating composite laminated cylindrical shells highly depends on the rotating speed of the shell [1–11], ply orientation [2,4,7,11], end conditions [4,5,9], and geometric variables of the shell such as thickness, length, and radius [2,4,6–10]. Therefore, proper selection of appropriate lamination to maximize the fundamental frequency of rotating composite laminated cylindrical shells becomes a crucial problem [12–16] and more research could be done in this area [17].

Research on the subject of structural optimization has been reported by many investigators [18]. Among various optimization schemes, the golden section method is a simple technique and can be easily programmed for solution on the computer [19,20]. In this investigation, maximization of the fundamental natural frequency of rotating laminated cylindrical shells with respect to fiber orientations is performed by using the golden section method. The fundamental frequencies of laminated cylindrical shells are calculated by using the ABAQUS finite element program [21]. In the paper, the constitutive equations for fiber-composite lamina, vibration analysis, and golden section method are briefly reviewed. The influence of rotating speed, end conditions, shell thickness, shell length, and shell radius on the maximum fundamental natural frequency and the associated optimal fiber orientations of the rotating laminated cylindrical shells is presented and important conclusions obtained from the study are given.

II. Constitutive Matrix for Fiber-Composite Laminae

In the finite element analysis, the laminated cylindrical shells are modeled by eight-node isoparametric shell elements with 6 degrees of freedom per node (three displacements and three rotations). The reduced integration rule together with hourglass stiffness control is employed to formulate the element stiffness matrix [21].

For fiber-composite laminated materials (Fig. 1), the stress–strain relations for a lamina in the material coordinates at an element integration point can be written as

$$\{\sigma'\} = [Q'_1]\{\varepsilon'\}, \qquad \{\tau'\} = [Q'_2]\{\gamma'\} \tag{1}$$

$$[Q'_1] = \begin{bmatrix} \frac{E_{11}}{1-\nu_{12}\nu_{21}} & \frac{\nu_{12}E_{22}}{1-\nu_{12}\nu_{21}} & 0 \\ \frac{\nu_{21}E_{11}}{1-\nu_{12}\nu_{21}} & \frac{E_{22}}{1-\nu_{12}\nu_{21}} & 0 \\ 0 & 0 & G_{12} \end{bmatrix} \qquad [Q'_2] = \begin{bmatrix} \alpha_1 G_{13} & 0 \\ 0 & \alpha_2 G_{23} \end{bmatrix} \tag{2}$$

The α_1 and α_2 are shear correction factors, which are calculated in ABAQUS by assuming that the transverse shear energy through the thickness of laminate is equal to that in unidirectional bending

Received 2 November 2006; revision received 4 April 2007; accepted for publication 25 April 2007. Copyright © 2007 by the American Institute of Aeronautics and Astronautics, Inc. All rights reserved. Copies of this paper may be made for personal or internal use, on condition that the copier pay the $10.00 per-copy fee to the Copyright Clearance Center, Inc., 222 Rosewood Drive, Danvers, MA 01923; include the code 0001-1452/07 $10.00 in correspondence with the CCC.

*Professor, Department of Civil Engineering and Sustainable Environment Research Center. Senior Member AIAA.

†Graduate Research Assistant, Department of Civil Engineering.

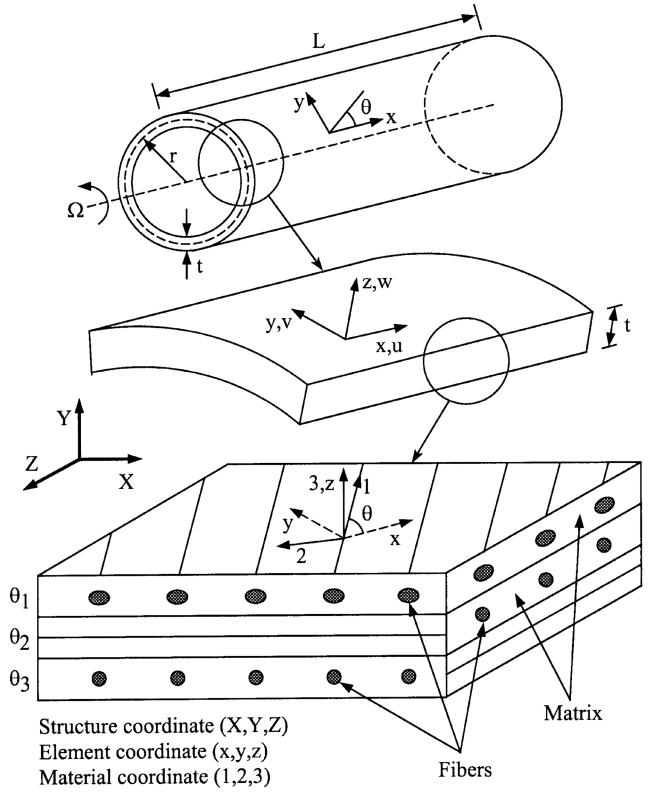

Fig. 1 Material, element, and structure coordinates of rotating fiber-composite laminated cylindrical shell.

[21,22]. The constitutive equations for the lamina in the element coordinates become

$$\{\sigma\} = [Q_1]\{\varepsilon\}, \qquad [Q_1] = [T_1]^T[Q_1'][T_1] \tag{3}$$

$$\{\tau\} = [Q_2]\{\gamma\}, \qquad [Q_2] = [T_2]^T[Q_2'][T_2] \tag{4}$$

$$[T_1] = \begin{bmatrix} \cos^2\theta & \sin^2\theta & \sin\theta\cos\theta \\ \sin^2\theta & \cos^2\theta & -\sin\theta\cos\theta \\ -2\sin\theta\cos\theta & 2\sin\theta\cos\theta & \cos^2\theta - \sin^2\theta \end{bmatrix}$$
$$[T_2] = \begin{bmatrix} \cos\theta & \sin\theta \\ -\sin\theta & \cos\theta \end{bmatrix} \tag{5}$$

The element coordinate system has the x, y, and z axes in the longitudinal direction, the circumferential direction, and the radial direction of the cylindrical shell, respectively (Fig. 1). If there are n layers in the layup, the stress resultants can be defined as

$$\begin{Bmatrix} \{N\} \\ \{M\} \\ \{V\} \end{Bmatrix} = \int_{-t/2}^{t/2} \begin{Bmatrix} \{\sigma\} \\ z\{\sigma\} \\ \{\tau\} \end{Bmatrix} \mathrm{d}z$$
$$= \sum_{j=1}^{n} \begin{bmatrix} (z_{jt}-z_{jb})[Q_1] & \frac{1}{2}\left(z_{jt}^2-z_{jb}^2\right)[Q_1] & [0] \\ \frac{1}{2}\left(z_{jt}^2-z_{jb}^2\right)[Q_1] & \frac{1}{3}\left(z_{jt}^3-z_{jb}^3\right)[Q_1] & [0] \\ [0]^T & [0]^T & (z_{jt}-z_{jb})[Q_2] \end{bmatrix} \begin{Bmatrix} \{\varepsilon_0\} \\ \{\kappa\} \\ \{\gamma\} \end{Bmatrix} \tag{6}$$

z_{jt} and z_{jb} are the distances from the midsurface of the section to the top and the bottom of the jth layer, respectively.

III. Vibration Analysis

For the free vibration analysis of an undamped structure, the equation of motion of the structure can be written in the following form [23]:

$$[M]\{\ddot{\boldsymbol{D}}\} + [K]\{\boldsymbol{D}\} = \{0\} \tag{7}$$

The $\{0\}$ is a zero vector. Since $\{\boldsymbol{D}\}$ undergoes harmonic motion, we can express

$$\{\boldsymbol{D}\} = \{\bar{\boldsymbol{D}}\}\sin\omega t; \qquad \{\ddot{\boldsymbol{D}}\} = -\omega^2\{\bar{\boldsymbol{D}}\}\sin\omega t \tag{8}$$

where the $\{\bar{\boldsymbol{D}}\}$ vector contains the amplitudes of the $\{\boldsymbol{D}\}$ vector. Then Eq. (7) can be written in an eigenvalue expression as

$$([K] - \omega^2[M])\{\bar{\boldsymbol{D}}\} = \{0\} \tag{9}$$

When a laminated cylindrical shell rotates at a constant speed about its axial direction, centrifugal forces are developed in the radial direction of the shell. The centrifugal forces can be treated as initial loads and cause initial stresses in the shell. Consequently, the stiffness matrix $[K]$ in Eq. (9) can be separated into two matrices as

$$[K] = [K_L] + [K_\sigma] \tag{10}$$

The $[K_L]$ is the traditional linear stiffness matrix and $[K_\sigma]$ is a geometric stress stiffness matrix due to the preload, that is, the centrifugal forces. Then Eq. (9) becomes

$$([K_L] + [K_\sigma] - \omega^2[M])\{\bar{\boldsymbol{D}}\} = \{0\} \tag{11}$$

The above equation is an eigenvalue expression. If $\{\bar{\boldsymbol{D}}\}$ is not a zero vector, we must have

$$|[K_L] + [K_\sigma] - \omega^2[M]| = 0 \tag{12}$$

In ABAQUS, a subspace iteration procedure [21] is used to solve for the natural frequency ω, and the eigenvectors (or vibration modes) $\{\bar{\boldsymbol{D}}\}$. The obtained smallest natural frequency (fundamental frequency) is then the objective function for maximization.

IV. Golden Section Method

We begin by presenting the golden section method [19,20] for determining the minimum of the unimodal function F, which is a function of the independent variable $\underline{X}$. It is assumed that lower bound $\underline{X}_L$ and upper bound $\underline{X}_U$ on $\underline{X}$ are known and the minimum can be bracketed (Fig. 2). In addition, we assume that the function has been evaluated at both bounds and the corresponding values are F_L

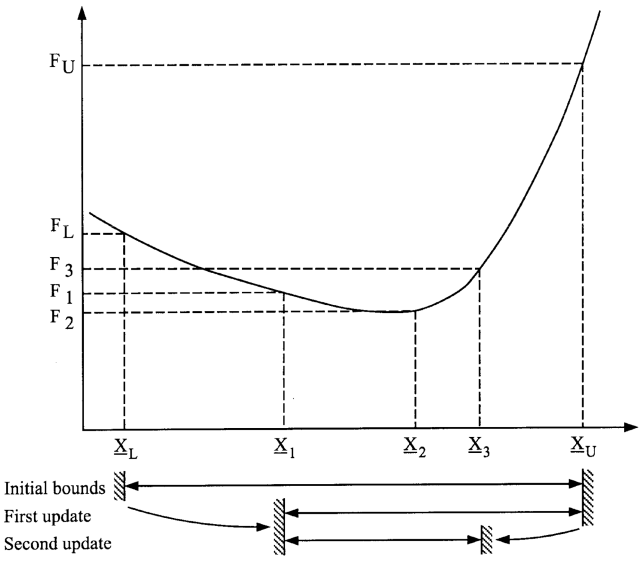

Fig. 2 The golden section method.

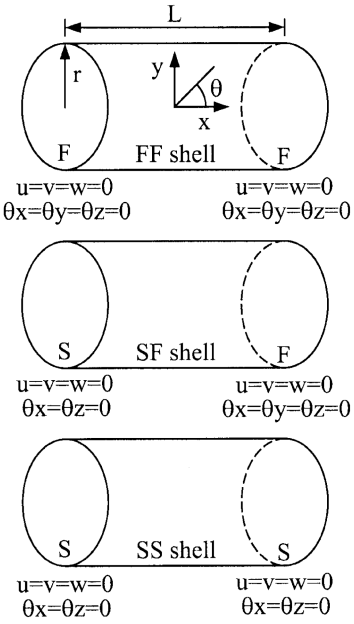

Fig. 3 Boundary conditions of cylindrical shells.

and F_U. Now we can pick up two intermediate points $\underline{X}_1$ and $\underline{X}_2$ such that $\underline{X}_1 < \underline{X}_2$ and evaluate the function at these two points to provide F_1 and F_2. Because F_1 is greater than F_2, now $\underline{X}_1$ forms a new lower bound and we have a new set of bounds, $\underline{X}_1$ and $\underline{X}_U$. We can now select an additional point, $\underline{X}_3$, for which we evaluate F_3. It is clear that F_3 is greater than F_2, so $\underline{X}_3$ replaces $\underline{X}_U$ as the new upper bound. Repeating this process, we can narrow the bounds to whatever tolerance is desired.

To determine the method for choosing the interior points $\underline{X}_1, \underline{X}_2, \underline{X}_3, \ldots$, we pick the values of $\underline{X}_1$ and $\underline{X}_2$ to be symmetric about the center of the interval and satisfying the following expressions:

$$\underline{X}_U - \underline{X}_2 = \underline{X}_1 - \underline{X}_L \tag{13}$$

$$\frac{\underline{X}_1 - \underline{X}_L}{\underline{X}_U - \underline{X}_L} = \frac{\underline{X}_2 - \underline{X}_1}{\underline{X}_U - \underline{X}_1} \tag{14}$$

Let τ be a number between 0 and 1. We can define the interior point $\underline{X}_1$ and $\underline{X}_2$ to be

$$\underline{X}_1 = (1 - \tau)\underline{X}_L + \tau \underline{X}_U \tag{15a}$$

$$\underline{X}_2 = \tau \underline{X}_L + (1 - \tau)\underline{X}_U \tag{15b}$$

Substituting Eqs. (15a) and (15b) into Eq. (14), we obtain

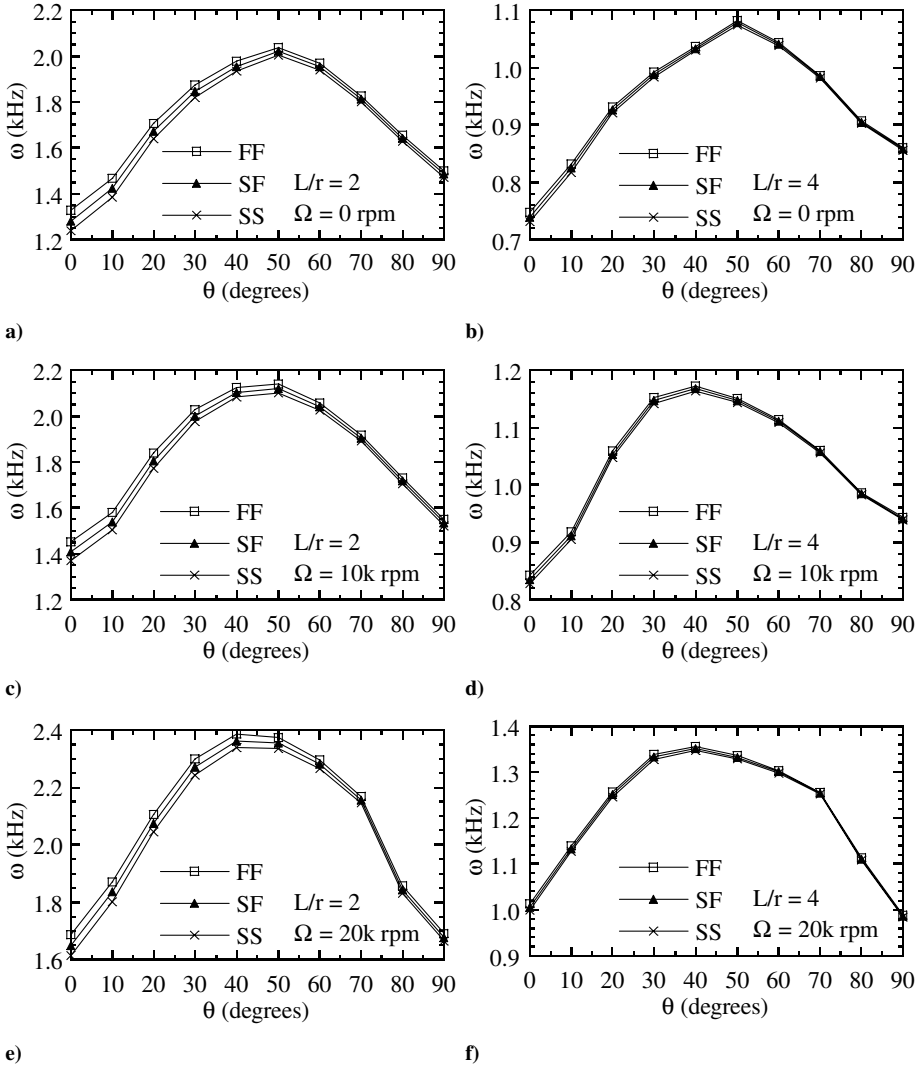

Fig. 4 Effect of end condition on fundamental frequency of thin $[\pm\theta/90/0]_{2s}$ laminated cylindrical shells ($r = 10$ cm).

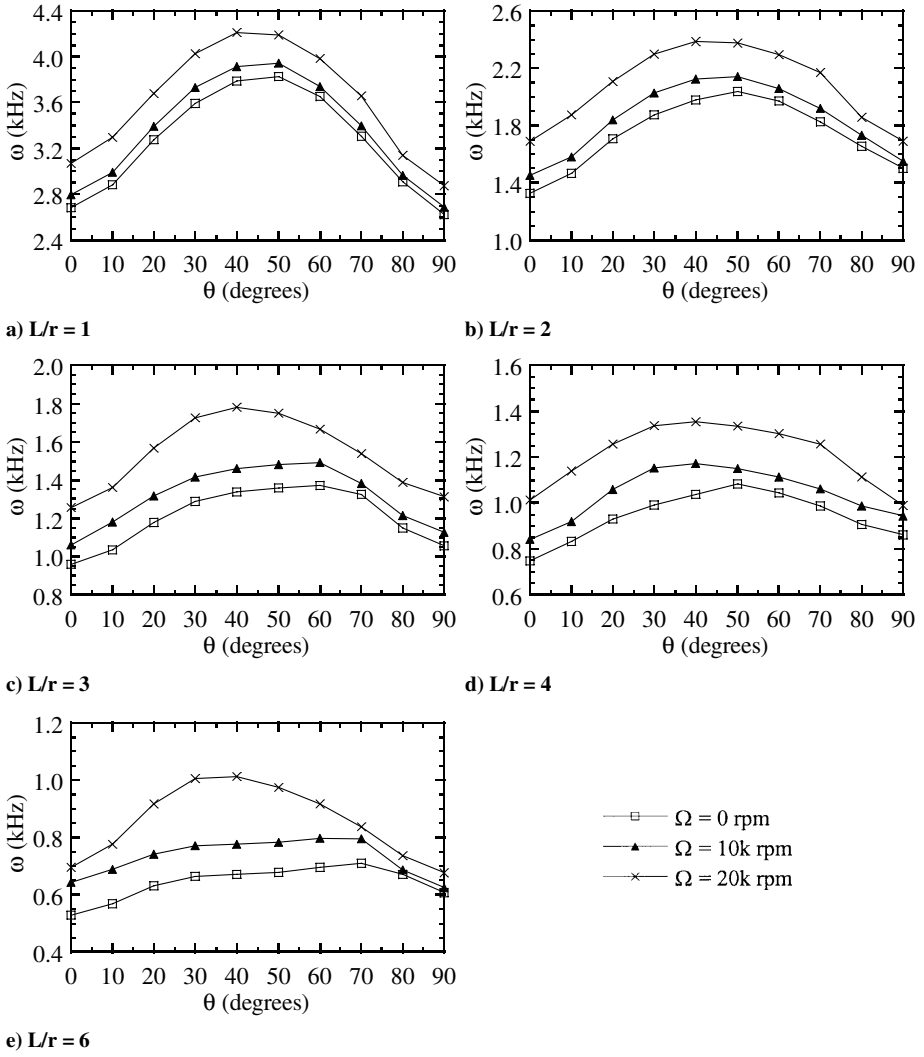

Fig. 5 Effect of the L/r ratio and rotating speed Ω on fundamental frequency of thin $[\pm\theta/90/0]_{2s}$ laminated cylindrical shells with two fixed ends ($r = 10$ cm).

$$\tau^2 - 3\tau + 1 = 0 \tag{16}$$

Solving the above equation, we obtain $\tau = 0.38197$. The ratio $(1 - \tau)/\tau = 1.61803$ is the famous "golden section" number. For a problem involving the estimation of the maximum of a one-variable function F, we need only minimize the negative of the function, that is, minimize $-F$.

V. Numerical Analysis

A. Accuracy of Shell Elements

Before the numerical analysis, the accuracy of the eight-node shell element has been verified by analyzing an isotropic cylindrical shell with free edges at both ends. The thickness of the shell is $t = 3.81$ cm, the length $L = 24.5$ cm, the radius $r = 9.525$ cm, and the rotating speed $\Omega = 50$ Hz. Young's modulus, Poisson's ratio, and density of the shell are $E = 207$ GPa, $\nu = 0.28$, and $\rho = 7860$ kg/m^3. The numerical solution obtained by the ABAQUS employing 640 eight-node shell elements (32 rows in the circumferential direction and 20 rows in the longitudinal direction) is $\omega = 2463$ s^{-1}, which is in good agreement with the result, $\omega = 2477$ s^{-1}, obtained by Guo et al. [24]. On the basis of this result and previous experience on the convergent studies of composite cylindrical shells [15,25], it is decided to use 160 (32×5), 320 (32×10), 480 (32×15), and 640 (32×20) elements to model the laminated cylindrical shells having L/r ratio equal to 1, 2, 3, and 6 for the following numerical analyses.

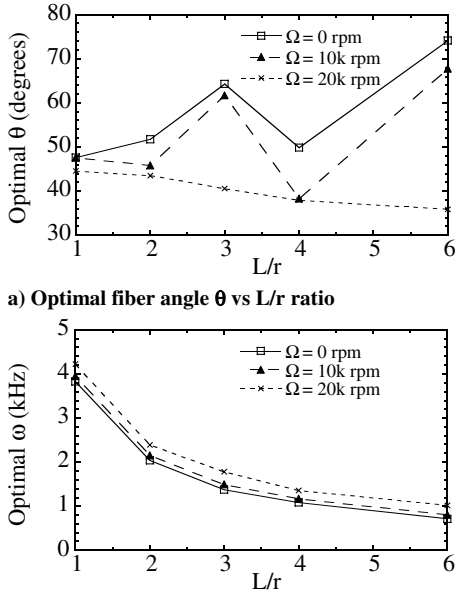

a) Optimal fiber angle θ vs L/r ratio

b) Optimal fundamental frequency ω vs L/r ratio

Fig. 6 Effect of the L/r ratio and rotating speed Ω on optimal fiber angle and optimal fundamental frequency of thin $[\pm\theta/90/0]_{2s}$ laminated cylindrical shells with two fixed ends ($r = 10$ cm).

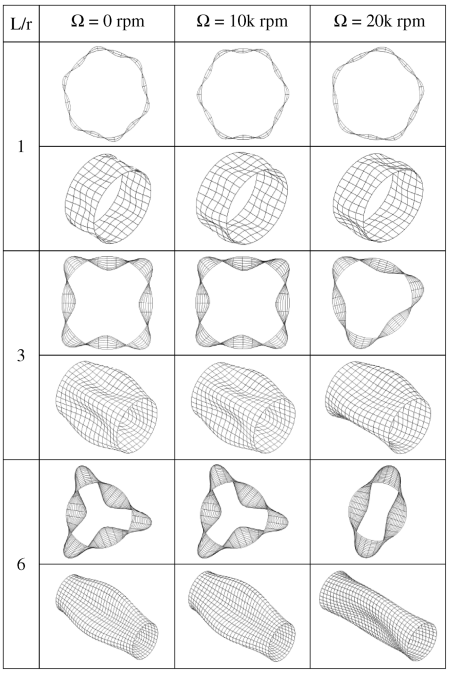

Fig. 7 Fundamental vibration mode of thin $[\pm\theta/90/0]_{2s}$ laminated cylindrical shells with two fixed ends and under optimal fiber angles ($r = 10$ cm).

B. Thin $[\pm\theta/90/0]_{2s}$ Laminated Cylindrical Shells with Various End Conditions, Lengths, and Rotating Speeds

In this section composite laminated cylindrical shells with three types of end conditions (Fig. 3) are considered, which are two ends fixed (denoted by FF), one end simply supported and the other end fixed (denoted by SF), and two ends simply supported (denoted by SS). These boundary conditions are specified in the local coordinate system of shell, in which x is the longitudinal direction, y the circumferential direction, and z the radial direction. The radius of the shell r is equal to 10 cm and the length of the shell L varies from 10 to 60 cm. The laminate layup of the shells is $[\pm\theta/90/0]_{2s}$ (16-ply thin shell) and the thickness of each ply is 0.125 mm. To study the influence of rotating speed on the results of optimization, $\Omega = 0$, 10,000, 20,000 rpm are selected for analysis. The lamina consists of graphite/epoxy and material constitutive properties are taken from Crawley [26], which are $E_{11} = 128$ GPa, $E_{22} = 11$ GPa, $\nu_{12} = 0.25$, $G_{12} = G_{13} = 4.48$ GPa, $G_{23} = 1.53$ GPa, and $\rho = 1500$ kg/m^3. In the analysis, no symmetry simplifications are made for those shells.

Figure 4 shows the fiber angle θ and the associated fundamental frequency ω for thin $[\pm\theta/90/0]_{2s}$ laminated cylindrical shells with various boundary conditions, L/r ratios, and rotating speeds. From Figs. 4b, 4d, and 4f, we can observe that the boundary conditions have almost no influence on the fundamental frequency of the laminated cylindrical shells with large L/r ratio (say $L/r = 4$). From Figs. 4a, 4c, and 4e, we can observe that the boundary conditions do have some influences on the fundamental frequency of the laminated cylindrical shells with small L/r ratio (i.e., $L/r = 2$). However,

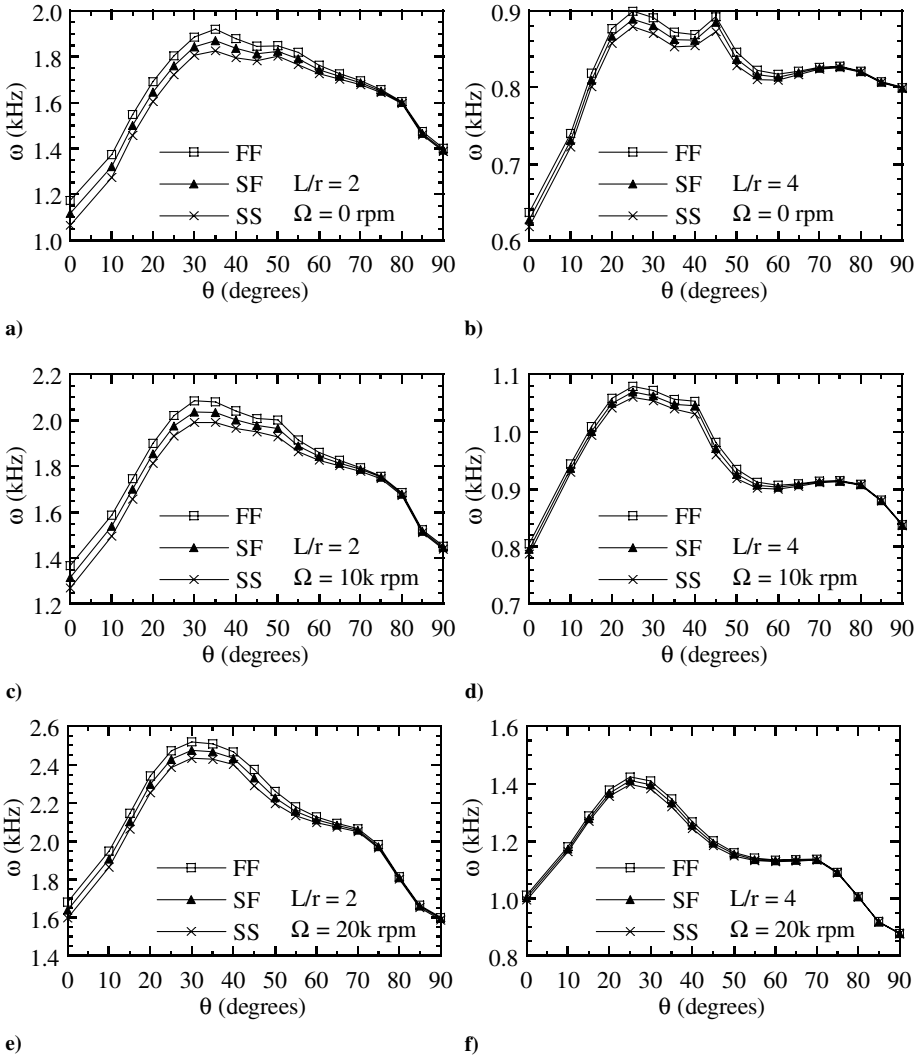

Fig. 8 Effect of end condition on fundamental frequency of thin $[\pm\theta]_{4s}$ laminated cylindrical shells ($r = 10$ cm).

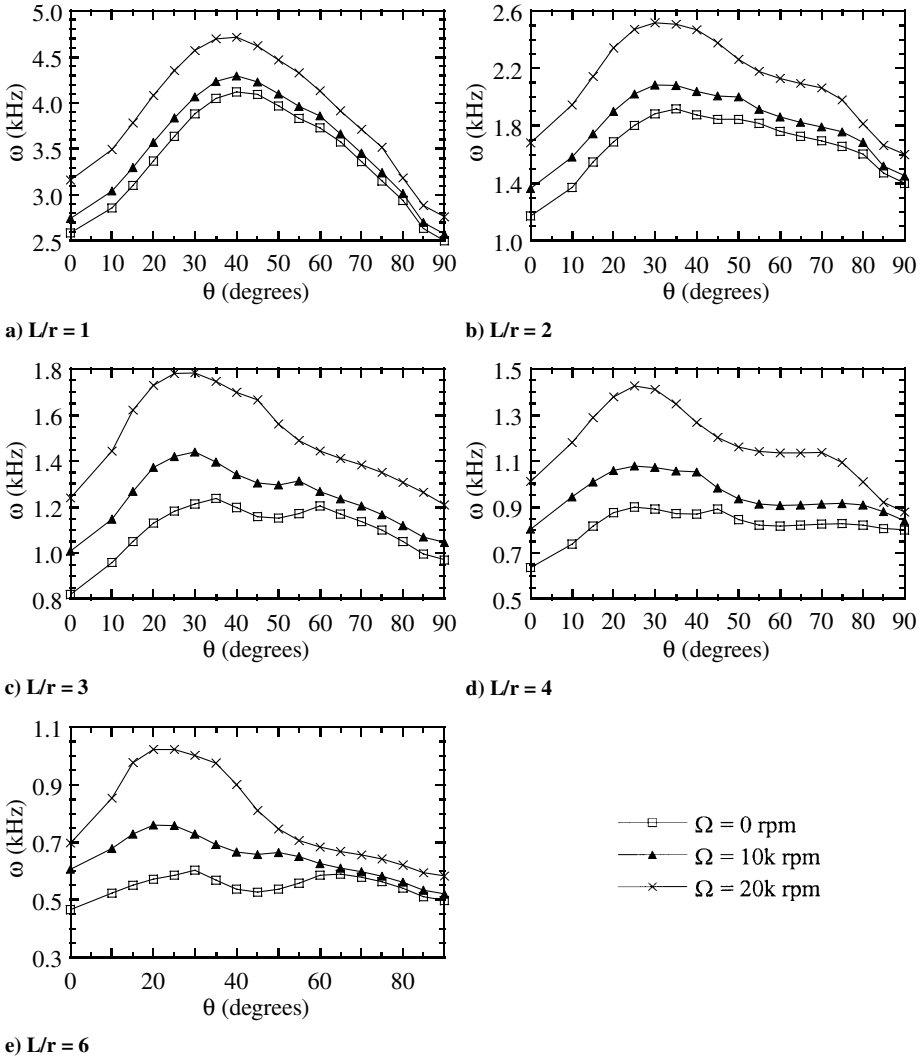

Fig. 9 Effect of the L/r ratio and rotating speed Ω on fundamental frequency of thin $[\pm\theta]_{4s}$ laminated cylindrical shells with two fixed ends ($r = 10$ cm).

these influences are rather insignificant. As a result, the remaining numerical analyses are focused on laminated cylindrical shells with two fixed ends only.

Figure 5 shows the effect of L/r ratio and rotating speed Ω on the fundamental frequency ω of thin $[\pm\theta/90/0]_{2s}$ laminated cylindrical shells with two fixed ends. It can be seen that the shells with higher rotating speed generally yield higher fundamental frequency. In addition, the shells with smaller L/r ratio usually render higher fundamental frequency too.

To find the optimal fiber angle θ and the associated optimal fundamental frequency ω, we can express the optimization problem as

$$\text{maximize}: \omega(\theta) \tag{17a}$$

$$\text{subjected to}: 0 \le \theta \le 90 \text{ deg} \tag{17b}$$

Before the golden section method is carried out, the fundamental frequency ω of the laminated cylindrical shell is calculated by employing the ABAQUS finite element program for every 10 deg increment in the θ angle to locate the maximum point approximately as shown by Fig. 5. Then proper upper and lower bounds are selected and the golden section method is performed. The optimization process is terminated when an absolute tolerance (the difference of the two intermediate points between the upper bound and the lower bound) $\Delta\theta \le 0.5$ deg is reached.

Figure 6 shows the optimal fiber angle θ and the associated optimal fundamental frequency ω versus the L/r ratio for thin $[\pm\theta/90/0]_{2s}$

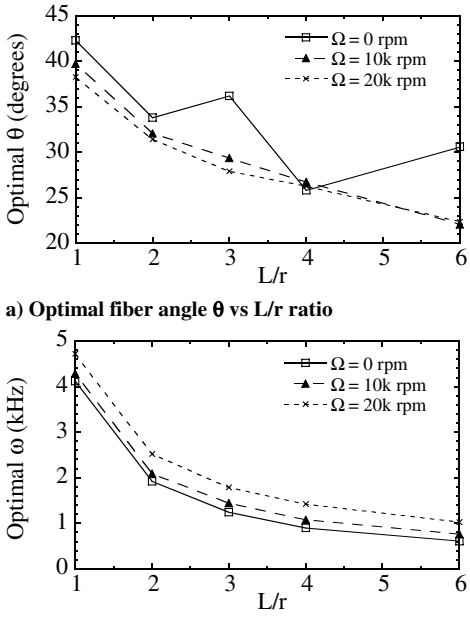

Fig. 10 Effect of the L/r ratio and rotating speed Ω on optimal fiber angle and optimal fundamental frequency of thin $[\pm\theta]_{4s}$ laminated cylindrical shells with two fixed ends ($r = 10$ cm).

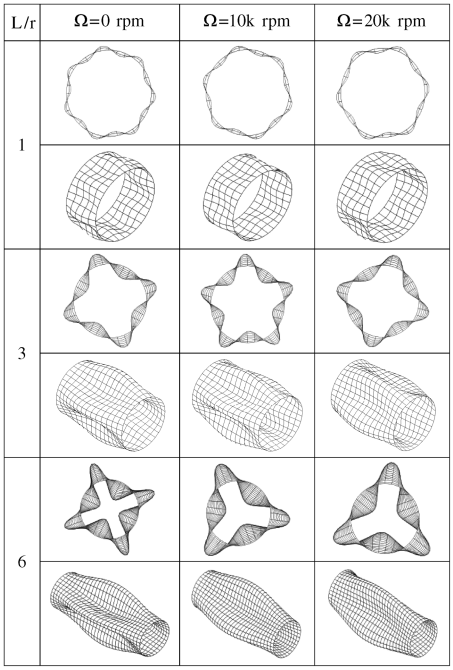

Fig. 11 Fundamental vibration mode of thin $[\pm\theta]_{4s}$ laminated cylindrical shells with two fixed ends and under optimal fiber angles ($r = 10$ cm).

laminated cylindrical shells. From Fig. 6a we can see that the optimal fiber angle θ of the cylindrical shell oscillates between 30 and 80 deg when the rotating speed of the shell is slow (say $\Omega \leq 10\text{k} \cdot \text{rpm}$). However, when the rotating speed of the shell is fast (say $\Omega = 10\text{k} \cdot \text{rpm}$), the optimal fiber angle θ of the cylindrical shell decreases monotonically with the increasing of the L/r ratio. Figure 6b shows that the optimal fundamental frequency ω decreases with the increasing of the L/r ratio. Under the same L/r ratio, the higher the rotating speed Ω, the higher the optimal fundamental frequency ω.

Figure 7 shows the fundamental vibration modes of thin $[\pm\theta/90/0]_{2s}$ laminated cylindrical shells with two fixed ends and under the optimal fiber orientation. We can find that when the rotating speed or the L/r ratio increases, the fundamental vibration modes of these cylindrical shells would have less waves in the circumferential direction. The reason for the mode switching is that the increase of the rotating speed or the L/r ratio weakens the stiffness of composite shell structures. Consequently, the oscillations in the results as shown in Fig. 6a might be due to the mode switching.

C. Thin $[\pm\theta]_{4s}$ Laminated Cylindrical Shells with Various End Conditions, Lengths, and Rotating Speeds

In this section, laminated cylindrical shells similar to the previous section are analyzed except that the laminate layup is changed to $[\pm\theta]_{4s}$. Figure 8 shows the fiber angle θ and the associated fundamental frequency ω for thin $[\pm\theta]_{4s}$ laminated cylindrical shells with various boundary condition, L/r ratio, and rotating speed Ω.

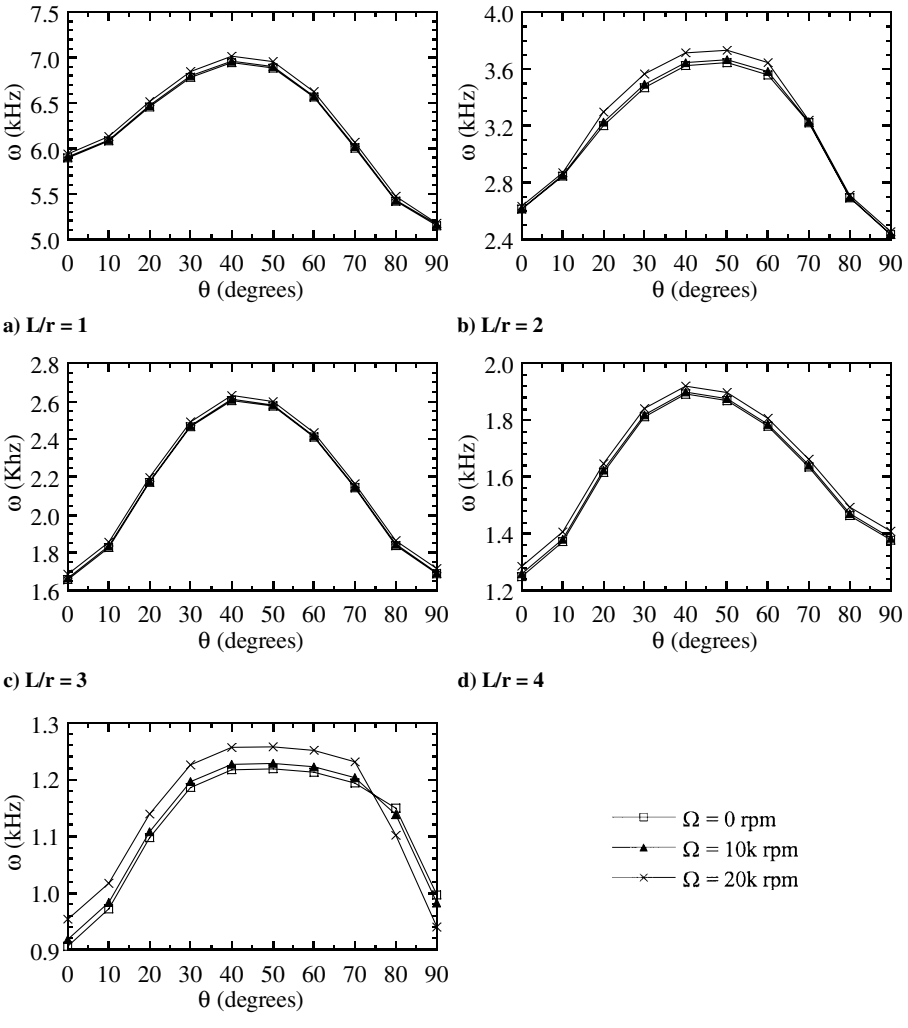

Fig. 12 Effect of the L/r ratio and rotating speed Ω on fundamental frequency of thick $[\pm\theta/90/0]_{10s}$ laminated cylindrical shells with two fixed ends ($r = 10$ cm).

Similar to the $[\pm\theta/90/0]_{2s}$ shells, the influences of boundary conditions on the fundamental frequency ω of the $[\pm\theta]_{4s}$ shells are rather insignificant. As a result, the remaining numerical analyses are focused on laminated cylindrical shells with two fixed ends only.

Figure 9 shows the effect of the L/r ratio and rotating speed Ω on the fundamental frequency ω of thin $[\pm\theta]_{4s}$ laminated cylindrical shells with two fixed ends. Again, the shells with higher rotating speed and with smaller L/r ratio generally yield higher fundamental frequency.

Figure 10 shows the optimal fiber angle θ and the associated optimal fundamental frequency ω versus the L/r ratio for thin $[\pm\theta]_{4s}$ laminated cylindrical shells. From Fig. 10a we can see that the optimal fiber angle θ of the cylindrical shell oscillates between 25 and 45 deg when the rotating speed of the shell is slow (say $\Omega < 10\text{k} \cdot \text{rpm}$). However, when the rotating speed of the shell is fast (say $\Omega \geq 10\text{k} \cdot \text{rpm}$), the optimal fiber angle θ of the cylindrical shell decreases monotonically with the increasing of the L/r ratio. Figure 10b shows that the optimal fundamental frequency ω decreases with the increasing of the L/r ratio. Again, under the same L/r ratio, the higher the rotating speed Ω, the higher the optimal fundamental frequency ω. Comparing Fig. 10a with Fig. 6a, we can find that under the same geometry and rotating speed, the optimal fiber angles of $[\pm\theta]_{4s}$ shells are usually smaller than those of $[\pm\theta/90/0]_{2s}$ shells. Comparing Fig. 10b with Fig. 6b, we can find that under the same geometry and rotating speed, the optimal fundamental frequencies of $[\pm\theta]_{4s}$ shells are slightly higher than those of $[\pm\theta/90/0]_{2s}$ shells.

Figure 11 shows the fundamental vibration modes of thin $[\pm\theta]_{4s}$ laminated cylindrical shells with two fixed ends and under the optimal fiber orientation. Again, when the rotating speed or the L/r ratio increases, the fundamental vibration modes of these cylindrical shells would have less waves in the circumferential direction. Comparing Fig. 11 with Fig. 7, we can observe that under the same geometry and rotating speed, the fundamental vibration modes of $[\pm\theta]_{4s}$ shells would have more waves in the circumferential direction than those of $[\pm\theta/90/0]_{2s}$ shells.

D. Thick $[\pm\theta/90/0]_{10s}$ Laminated Cylindrical Shells with Various Lengths and Rotating Speeds

In this section, laminated cylindrical shells similar to previous sections are analyzed except that the laminate layup is changed to $[\pm\theta/90/0]_{10s}$. Figure 12 shows the effect of the L/r ratio and rotating speed Ω on the fundamental frequency ω of thick $[\pm\theta/90/0]_{10s}$ laminated cylindrical shells with two fixed ends. Again, the shells with higher rotating speed and with smaller L/r ratio generally yield higher fundamental frequency. Comparing Fig. 12 with Fig. 5, we can see that the influence of the rotating speed on the fundamental frequency of thick laminated cylindrical shells is insignificant especially when the L/r ratio is small.

Figure 13 shows the optimal fiber angle θ and the associated optimal fundamental frequency ω versus the L/r ratio for thick $[\pm\theta/90/0]_{10s}$ laminated cylindrical shells. From this figure we can see that the influence of rotating speed on the optimal fiber angle as well as the associated optimal fundamental frequency is very small. Comparing Fig. 13b with Fig. 6b, we can find out that the optimal fundamental frequencies of thick shells are approximately twice as high as those of thin shells.

Figure 14 shows the fundamental vibration modes of thick $[\pm\theta/90/0]_{10s}$ laminated cylindrical shells with two fixed ends and under the optimal fiber orientation. It can be seen that the fundamental vibration modes of the shells would have less waves in the circumferential direction when the L/r ratio is large. However, the fundamental vibration modes of these thick shells are insensitive to the rotating speed. Figure 15 shows the increase of the optimal fundamental frequency (compared to the same shell with no rotating speed) versus the L/r ratio for $[\pm\theta/90/0]_{2s}$ and $[\pm\theta/90/0]_{10s}$ shells. We can see that the increase of the fundamental frequency is rather

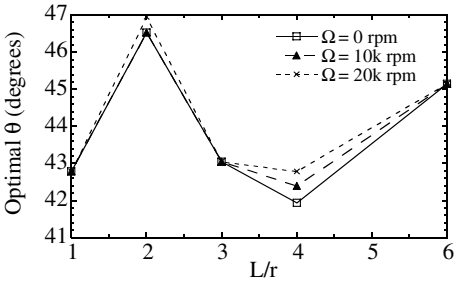

a) Optimal fiber angle θ vs L/r ratio

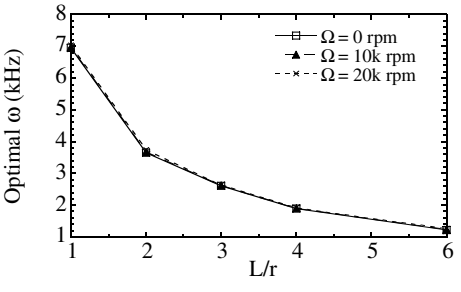

b) Optimal fundamental frequency ω vs L/r ratio

Fig. 13 Effect of the L/r ratio and rotating speed Ω on optimal fiber angle and optimal fundamental frequency of thick $[\pm\theta/90/0]_{10s}$ laminated cylindrical shells with two fixed ends ($r = 10$ cm).

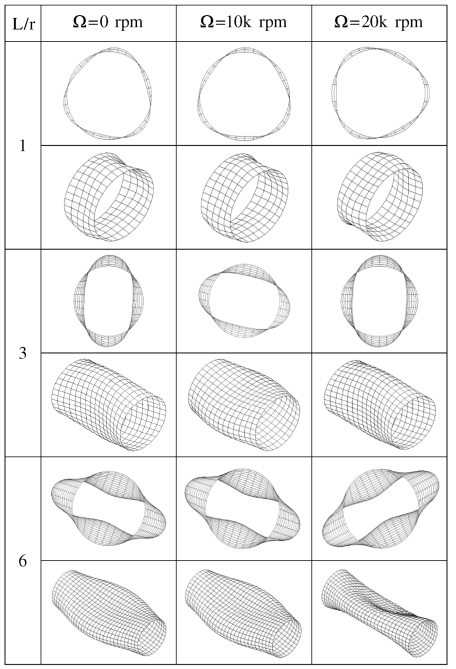

Fig. 14 Fundamental vibration mode of thick $[\pm\theta/90/0]_{10s}$ laminated cylindrical shells with two fixed ends and under optimal fiber angles ($r = 10$ cm).

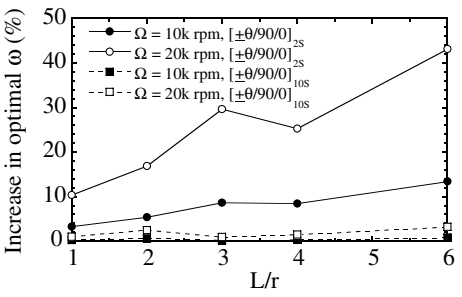

Fig. 15 Increase due to rotating speed of optimal fundamental frequency ω versus the L/r ratio for $[\pm\theta/90/0]_{2s}$ and $[\pm\theta/90/0]_{10s}$ laminated cylindrical shells with two fixed ends ($r = 10$ cm).

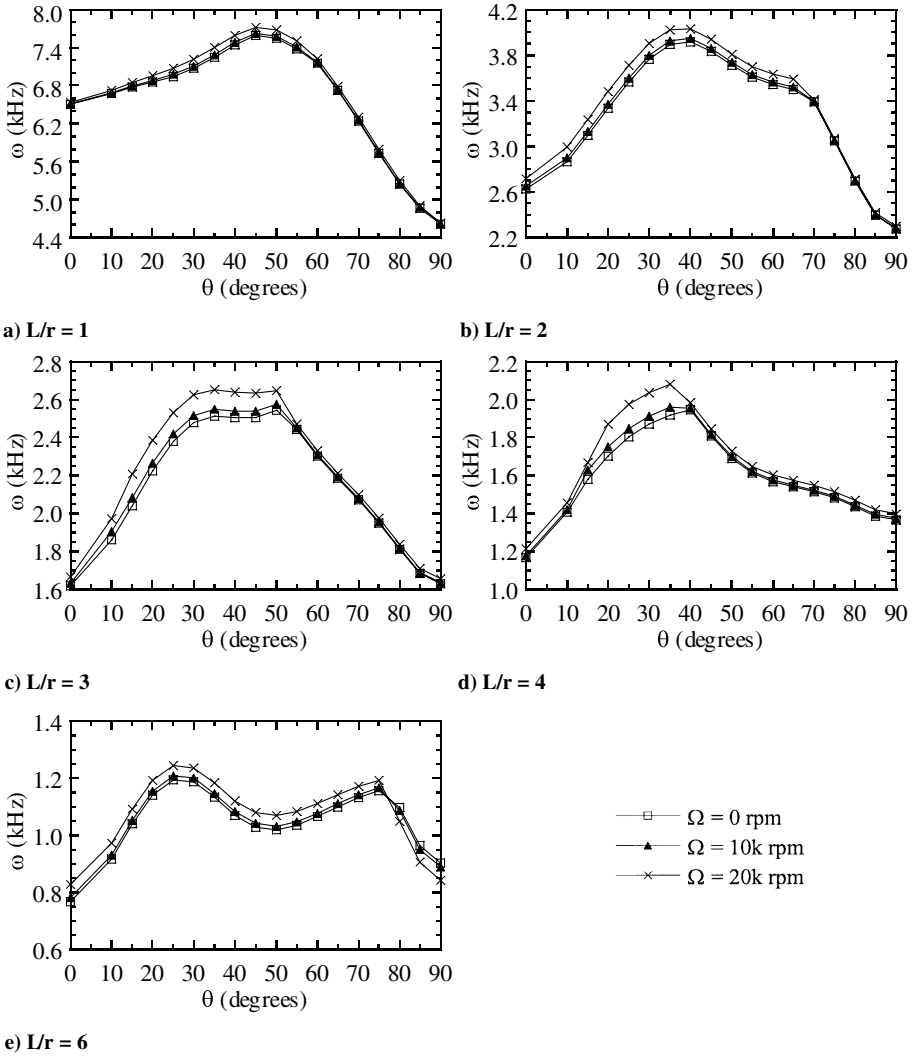

Fig. 16 Effect of the L/r ratio and rotating speed Ω on fundamental frequency of thick $[\pm\theta]_{20s}$ laminated cylindrical shells with two fixed ends ($r = 10$ cm).

small for thick $[\pm\theta/90/0]_{10s}$ shells. On the other hand, the increase of the fundamental frequency is significant for thin $[\pm\theta/90/0]_{2s}$ shells especially when the rotating speed is large (say 43% increase in optimal fundamental frequency for a shell with $L/r = 6$ and $\Omega = 20\text{k} \cdot \text{rpm}$).

E. Thick $[\pm\theta]_{20s}$ Laminated Cylindrical Shells with Various Lengths and Rotating Speeds

In this section, laminated cylindrical shells similar to previous sections are analyzed except that the laminate layup is changed to $[\pm\theta]_{20s}$. Figure 16 shows the effect of the L/r ratio and rotating speed Ω on the fundamental frequency ω of thick $[\pm\theta]_{20s}$ laminated cylindrical shells with two fixed ends. Again, the shells with higher rotating speed and with smaller L/r ratio generally yield higher fundamental frequency. Comparing Fig. 16 with Fig. 9, we can also observe that the influence of rotating speed on the fundamental frequency of thick laminated cylindrical shells is insignificant especially when the L/r ratio is small.

Figure 17 shows the optimal fiber angle θ and the associated optimal fundamental frequency ω versus the L/r ratio for thick $[\pm\theta]_{20s}$ laminated cylindrical shells. From Fig. 17a, we can see that the influence of rotating speed on the optimal fiber angle is small when the rotating speed of the shell is slow (say $\Omega \leq 10\text{k} \cdot \text{rpm}$). Nevertheless, the optimal fundamental frequency ω is insensitive to the rotating speed as shown by Fig. 17b. Comparing Fig. 17a with Fig. 10a, we can find that the optimal fiber angles of $[\pm\theta]_{20s}$ shells are usually larger than those of $[\pm\theta]_{4s}$ shells. Comparing Fig. 17b with

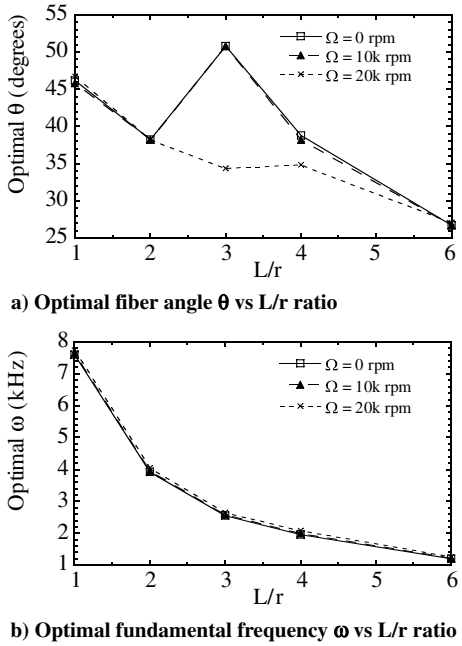

a) Optimal fiber angle θ vs L/r ratio

b) Optimal fundamental frequency ω vs L/r ratio

Fig. 17 Effect of the L/r ratio and rotating speed Ω on optimal fiber angle and optimal fundamental frequency of thick $[\pm\theta]_{20s}$ laminated cylindrical shells with two fixed ends ($r = 10$ cm).

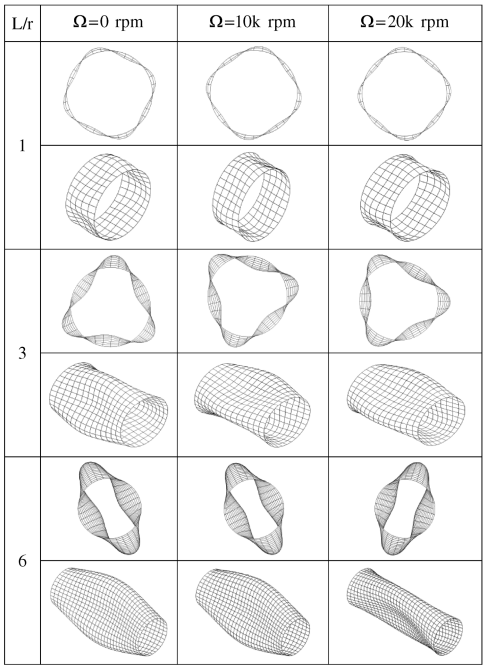

Fig. 18 Fundamental vibration mode of thick $[\pm\theta]_{20s}$ laminated cylindrical shells with two fixed ends and under optimal fiber angles ($r = 10$ cm).

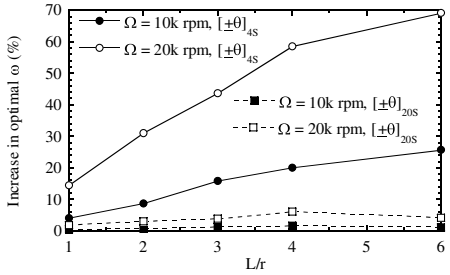

Fig. 19 Increase due to rotating speed of optimal fundamental frequency ω versus the L/r ratio for $[\pm\theta]_{4s}$ and $[\pm\theta]_{20s}$ laminated cylindrical shells with two fixed ends ($r = 10$ cm).

Fig. 10b, we find that the optimal fundamental frequencies of thick shells are again about twice as high as those of thin shells.

Figure 18 shows the fundamental vibration modes of thick $[\pm\theta]_{20s}$ laminated cylindrical shells with two fixed ends and under the optimal fiber orientation. It can be seen that the fundamental vibration modes of the shells would have less waves in the circumferential direction when the L/r ratio is large. However, the fundamental vibration modes of these thick shells are insensitive to the rotating speed. Figure 19 shows the increase of the optimal fundamental frequency (compared to the same shell with no rotating speed) versus the L/r ratio for $[\pm\theta]_{4s}$ and $[\pm\theta]_{20s}$ shells. We can see that the increase of the fundamental frequency is rather small again for thick $[\pm\theta]_{20s}$ shells. On the other hand, the increase of the fundamental frequency is significant for thin $[\pm\theta]_{4s}$ shells especially when the rotating speed is large (say 69% increase in optimal fundamental frequency for shells with $L/r = 6$ and $\Omega = 20\text{k} \cdot \text{rpm}$).

VI. Conclusions

Based on the numerical results of this investigation, the following conclusions may be drawn:

1) The boundary conditions have very little influence on the fundamental frequency of the laminated cylindrical shells with large L/r ratio, though the boundary conditions do have some influence on the numerical results for the laminated cylindrical shells with small L/r ratio. However, these influences are really insignificant.

2) The laminated cylindrical shells with higher rotating speed and with smaller L/r ratio generally yield higher fundamental frequency.

3) Rotating speed has more influence on the optimal fiber angle and optimal fundamental frequency of thin $[\pm\theta/90/0]_{2s}$ and $[\pm\theta]_{4s}$ laminated cylindrical shells. On the other hand, rotating speed has less influence on the optimal fiber angle and optimal fundamental frequency of thick $[\pm\theta/90/0]_{10s}$ and $[\pm\theta]_{20s}$ laminated cylindrical shells.

4) When the L/r ratio increases, the fundamental vibration modes of both thin and thick cylindrical shells would have less waves in the circumferential direction. In addition, when the rotating speed increases, the fundamental vibration modes of thin cylindrical shells also would have less waves in the circumferential direction. The reason for the mode switching is that the increase of the L/r ratio or the rotating speed weakens the stiffness of composite shell structures. Consequently, many of the oscillations in the results might be due to the mode switching. On the other hand, the fundamental vibration modes of thick cylindrical shells are insensitive to the rotating speed.

Acknowledgment

This research work was financially supported by the National Science Council, Republic of China, under Grant NSC 92-2211-E-006-072.

References

[1] Kim, C. D., and Bert, C. W., "Critical Speed Analysis of Laminated Composite, Hollow Drive Shafts," *Composite Engineering*, Vol. 3, Nos. 7–8, 1993, pp. 633–643.

[2] Rand, O., and Stavsky, Y., "Response and Eigenfrequencies of Rotating Composite Cylindrical Shells," *Journal of Sound and Vibration*, Vol. 192, No. 1, 1996, pp. 65–77.

[3] Tylikowski, A., "Dynamic Stability of Rotating Composite Shafts," *Mechanics Research Communications*, Vol. 23, No. 2, 1996, pp. 175–180.

[4] Chen, L.-W., and Peng, W.-K., "The Stability Behavior of Rotating Composite Shafts Under Axial Compressive Loads," *Composite Structures*, Vol. 41, Nos. 3–4, 1998, pp. 253–263.

[5] Lam, K. Y., and Loy, C. T., "Influence of Boundary Conditions for a Thin Laminated Rotating Cylindrical Shells," *Composite Structures*, Vol. 41, Nos. 3–4, 1998, pp. 215–228.

[6] Lam, K. Y., and Wu, Q., "Vibrations of Thick Rotating Laminated Composite Cylindrical Shells," *Journal of Sound and Vibration*, Vol. 225, No. 3, 1999, pp. 483–501.

[7] Lee, Y.-S., and Kim, Y.-W., "Nonlinear Free Vibration Analysis of Rotating Hybrid Cylindrical Shells," *Computers and Structures*, Vol. 70, No. 2, 1999, pp. 161–168.

[8] Kadivar, M. H., and Samani, K., "Free Vibration of Rotating Thick Composite Cylindrical Shells Using Layerwise Laminate Theory," *Mechanics Research Communications*, Vol. 27, No. 6, 2000, pp. 679–684.

[9] Zhang, X. M., "Parametric Analysis of Frequency of Rotating Laminated Composite Cylindrical Shells with the Wave Propagation Approach," *Computer Methods in Applied Mechanics and Engineering*, Vol. 191, Nos. 19–20, 2002, pp. 2029–2043.

[10] Zhao, X., Liew, K. M., and Ng, T. Y., "Vibrations of Rotating Cross-Ply Laminated Circular Cylindrical Shells with Stringer and Ring Stiffeners," *International Journal of Solids and Structures*, Vol. 39, No. 2, 2002, pp. 529–545.

[11] Chang, C. Y., Chang, M. Y., and Huang, J. H., "Vibration Analysis of Rotating Composite Shafts Containing Randomly Oriented Reinforcements," *Composite Structures*, Vol. 63, No. 1, 2004, pp. 21–32.

[12] Raouf, R. A., "Tailoring the Dynamic Characteristics of Composite Panels Using Fiber Orientation," *Composite Structures*, Vol. 29, No. 3, 1994, pp. 259–267.

[13] Abrate, S., "Optimal Design of Laminated Plates and Shells," *Composite Structures*, Vol. 29, No. 3, 1994, pp. 269–286.

[14] Hu, H.-T., and Juang, C.-D., "Maximization of the Fundamental Frequencies of Laminated Curved Panels Against Fiber Orientation," *Journal of Aircraft*, Vol. 34, No. 6, 1997, pp. 792–801.

[15] Hu, H.-T., and Tsai, J.-Y., "Maximization of the Fundamental Frequencies of Laminated Cylindrical Shells with Respect to Fiber Orientations," *Journal of Sound and Vibration*, Vol. 225, No. 4, 1999, pp. 723–740.

[16] Hu, H.-T., and Ou, S.-C., "Maximization of the Fundamental Frequencies of Laminated Truncated Conical Shells with Respect to Fiber Orientations," *Composite Structures*, Vol. 52, Nos. 3–4, 2001, pp. 265–275.
[17] Bert, C. W., "Literature Review—Research on Dynamic Behavior of Composite and Sandwich Plates-V: Part 2," *The Shock and Vibration Digest*, Vol. 23, No. 7, 1991, pp. 9–21.
[18] Schmit, L. A., "Structural Synthesis—Its Genesis and Development," *AIAA Journal*, Vol. 19, No. 10, 1981, pp. 1249–1263.
[19] Vanderplaats, G. N., *Numerical Optimization Techniques for Engineering Design with Applications*, McGraw–Hill, New York, 1984, Chap. 2.
[20] Haftka, R. T., Gürdal, Z., and Kamat, M. P., *Elements of Structural Optimization*, 2nd revised edition, Kluwer Academic, Norwell, MA, 1990, Chap. 4.
[21] ABAQUS, Inc., ABAQUS Analysis User's Manuals and Example Problems Manuals, Ver. 6.6, Providence, RI, 2006.
[22] Whitney, J. M., "Shear Correction Factors for Orthotropic Laminates Under Static Load," *Journal of Applied Mechanics*, Vol. 40, No. 1, 1973, pp. 302–304.
[23] Cook, R. D., Malkus, D. S., Plesha, M. E., and Witt, R. J., *Concepts and Applications of Finite Element Analysis*, 4th ed., Wiley, New York, 2002.
[24] Guo, D., Chu, F. L., and Zheng, Z. C., "The Influence of Rotation on Vibration of a Thick Cylindrical Shell," *Journal of Sound and Vibration*, Vol. 242, No. 3, 2001, pp. 487–505.
[25] Wang, K.-L., "Optimization of Fundamental Frequencies of Rotating Laminated Cylindrical Shells," M.S. Thesis, Department of Civil Engineering, National Cheng-Kung University, Tainan, Taiwan, ROC, 2004.
[26] Crawley, E. F., "The Natural Modes of Graphite/Epoxy Cantilever Plates and Shells," *Journal of Composite Materials*, Vol. 13, No. 3, 1979, pp. 195–205.

J. Samareh
Associate Editor